Reliable full-field reconstruction of Lamb waves with shearography

Garza-Soto, Luis; Yue, Nan

DOI
10.1117/12.3062415

Publication date
2025

Document Version
Final published version

Published in
Optical Measurement Systems for Industrial Inspection XIV

Reliable full-field reconstruction of Lamb waves with shearography

Luis Garza-Soto[1,*], Nan Yue[1], and Andrei Anisimov[1]

[1]Department of Aerospace Structures and Materials, Delft University of Technology, Kluyverweg 1, 2629 HS, Delft, The Netherlands

ABSTRACT

Stroboscopic shearography techniques, including double pulse shearography, are able to image transient Lamb waves to support non-destructive testing of structures and materials. The amplitude of the signal measured with these techniques is known to depend on optical shear distance and direction but the experimental demonstrations presented in the literature are limited. We present improved experimental results that show the dependence of signal amplitude on shear distance. By carefully selecting the shear distance, we are able to visualize a defect with shearographic measurement of transient Lamb waves.

Keywords: Stroboscopic shearography, Double pulse shearography, Lamb wave imaging, Non-destructive testing

1. INTRODUCTION

Full-field imaging and mapping of ultrasonic waves acquired with non-destructive testing (NDT) techniques is useful for understanding wave propagation in specific materials and for detecting defects. Techniques like Ultrasonic Lamb Wave Tomography and Scanning Laser Doppler Vibrometry (SLDV) produce reliable maps but require multiple measurements or scanning.[1–4] Some optical techniques based on interference, mainly holography and shearography, are able to avoid this shortcoming and quickly obtain phase maps of transient Lamb waves over an extended area.[5–8] However, these full-field optical techniques have a lower signal to noise ratio (SNR) than Scanning Laser Doppler Vibrometry (SLDV) and it is of interest to improve their performance.[9]

The phase of the recorded interferograms can be obtained through temporal or spatial phase shifting. In temporal phase shifting, also known as temporal phase stepping, the interference is recorded at three or more phase conditions and the set of interferograms is used to calculate the phase of the electric field.[10,11] In spatial phase shifting, specifically with the Fourier transform method, the phase of the field gets encoded in a spatial carrier and is recovered through Fourier analysis.[12] The former is a standard in interferometry because of it's simplicity and the latter is especially useful for dynamic measurements because only one interferogram is captured at each deformation state.[13,14]

Transient Lamb waves have been observed with holographic and shearographic methods that use stroboscopic illumination in the form of a double pulse. Holographic techniques use a reference beam which is combined with the speckle pattern field to produce an interferogram,[5,6] and shearographic techniques use the interference of two speckle patterns sheared with respect to each other.[7,8] Some authors use several strobes synchronized with repeated acoustic excitation to obtain two states of surface displacement that are frozen at the times of the illumination laser pulses.[15–17] We present optical phase maps corresponding to transient Lamb waves observed with different values of the shear distance obtained through double pulse shearography, demonstrate the impact of this parameter on signal amplitude. Additionally, we show that the proper choice of shear distance can enhance visibility of defects if present.

Author contact: l.a.garzasoto@tudelft.nl

Optical Measurement Systems for Industrial Inspection XIV, edited by Peter Lehmann, Wolfgang Osten, Armando Albertazzi Gonçalves, Proc. of SPIE Vol. 13567, 135670O 2025 Published by SPIE · 0277-786X · doi: 10.1117/12.3062415

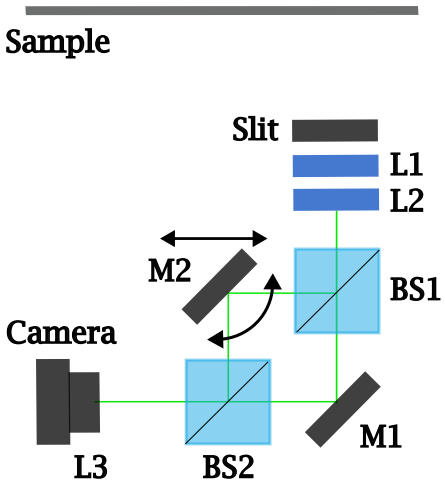

Figure 1. Schematic of the shearing device in our instrument. The sample is included as a reminder that the light source of the setup corresponds to the light scattered.

2. EXPERIMENT

An optical system was designed and built to be able to visualize transient Lamb waves with shearography. The illumination is provided by an INNOLAS Spitlight 600 Nd:YAG pulsed laser operating in double pulse mode. This mode allows us to obtain two sub pulses of 7 ns width from one flash lamp pulse of 200 μs width through the use of a pockels cell for Q-switching. The light beam passes through a negative lens and a ground glass diffuser to illuminate the area corresponding to the field of view at a distance of 1 m of approximately 18 x 18 cm.

The light scattered by the sample passes through our shearing device, the Mach-Zehnder interferometer shown in Fig. 1. A small fraction of the light scattered by the sample passes through an aperture and a couple of lenses (L1, L2) before entering the first beam spliter (BS1). The aperture is chosen to be a vertical slit to function as a spatial filter in the direction of shear that lets through as much light as possible and it is positioned at the front focal length of L1.[18] Approximately collimated light that was split at BS1 is reflected on a fixed mirror, M1, and a mirror that can be displaced in one direction and tilted, M2. Spatial carrier frequency and shear are determined by the combination of position and tilt of M2. For our specific alignment, displacement results exclusively on a change of spatial carrier frequency and tilt results on a change of both spatial carrier frequency and shear.[19] Thus, we control the shear distance and keep spatial carrier frequency fixed through a combination of displacement and tilt of M2. Light reflected on M1 and M2 is combined at BS2 and the interference is captured in one output of the interferometer by an IMPERX B3420 camera in double frame mode with a mounted imaging lens (L3).

A flat aluminium specimen is acoustically excited by a PZT transducer glued to the back side of the specimen. The signal is programmed in Keysight BenchLink Waveform Builder and sent to a Keysight 33220A Arbitrary Waveform Generator. The signal generator's output is connected to a WMA-300 high voltage amplifier and the output of the amplifier is connected to the PZT. We programmed 9 cycles of a sine wave multiplied by a gaussian curve to send a signal that approximates the behavior considered by our model. A second PZT is glued to the specimen and the excitation signal is monitored with a picoscope 6402A oscilloscope for verification purposes. We keep track of the signal before amplification, the signal received by the PZT, and the timing of the illumination. This simplifies the synchronization of the laser pulses, the PZT excitation, and the image acquisition, programmed with a real time synchronisation FPGA-based unit NI cRIO-9030.

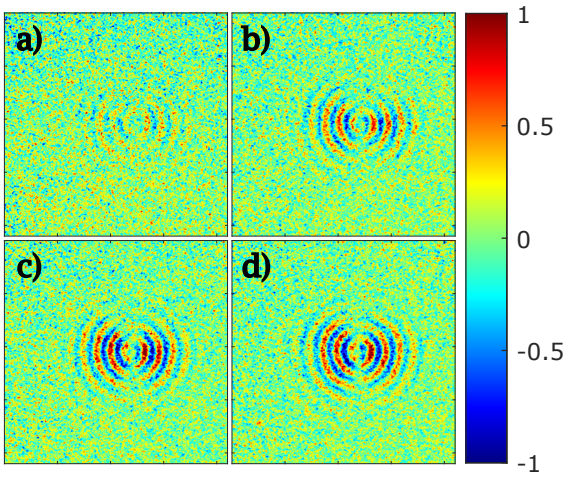

Figure 2. Phase maps corresponding to values of shear of a) 1 mm, b) 2.4 mm, c) 3.85 , and d) 5.3 mm. The amplitude of the measured signal is significantly greater when the shear distance is approximately half the spatial period of the acoustic waves, which in this case is measured to be 9.3 mm.

3. RESULTS

A single measurement with our instrument consists of a controlled sequence of illumination, PZT excitation, and acquisition of interferograms. Triggers are sent to the camera and to the wave generator before the trigger of the flashlamp, which generates two sub pulses used for illumination through Q-switching, since it takes some time to start acquisition and for the wave to propagate. The exact timing for the camera and wave generator triggers is chosen depending on which moment of the Lamb wave propagation we are interested in recording. Two interferograms are captured by the camera and saved to the computer.

The Fourier transform of the interferograms has three vertical sections that are well separated because of the spatial carrier and the vertical slit. The information of one of the side terms is filtered by multiplying by a Hann window mask and shifted to the center of the image, equivalent to subtracting the spatial carrier frequency.[12] The phase maps of both states obtained through the inverse Fourier transform are subtracted and the resulting phase map has the information of the optical phase change due to the propagation of the Lamb waves. The image is filtered using median and averaging filters with intermediate phase calculation.

To the best of our knowledge, there is no experimental confirmation in the literature of the variation of differential displacement amplitude while capturing Lamb waves with changing shear, other than implicitly in the displacements at different acoustic frequencies. Our experiments aim to clearly show the dependence on this parameter. Figure 2 shows the phase maps obtained from Lamb waves generated at 200 KHz excitation frequency with 200 V_{pp} and 1μs time between pulses. The phase maps correspond to measurements with different values of shear distance from 1 mm to 5.3 mm in four equal steps. We do not measure a phase map for the condition of no shear distance since this displacement is required for the technique. The phase maps have maximum amplitude when the spatial shift is closer to half the spatial period of the acoustic waves, an acoustic wave phase of π, at δx =5.3 mm.

If we would change the frequency of excitation, the wavelength of the propagating Lamb waves would change according to the dispersion equations and this means a change of the spatial frequency of the acoustic wave. Since the amount of phase in the acoustic wave depends on the spatial frequency and the shear distance, the maximum amplitude of the measured signal is expected at a different value of shear distance. The same effect is present in defects like flat bottom holes, where a change of local thickness results in a change of wavelength and spatial frequency. This allows us to set up a shear distance that matches the optimal condition in the area of the defect. Figure 3 shows transient Lamb waves in the presence of a defect. The shear distance parameter, δx, multiplied by the spatial frequency, $k = \frac{2\pi}{\lambda}$, is closer to π at the defect, $\lambda \approx 2\delta x$, increasing the signal amplitude.[20]

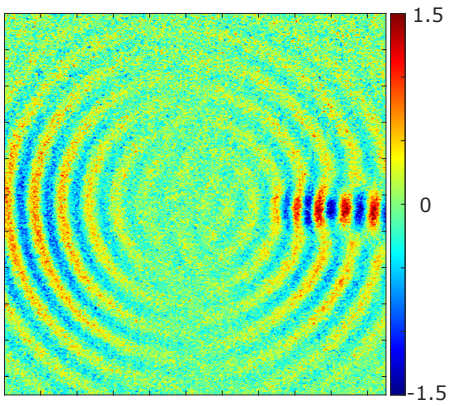

Figure 3. Transient Lamb waves in the presence of a defect. The shear distance matches the spatial frequency of the acoustic wave better at the defect than elsewhere.

REFERENCES

[1] Zhao, X., Royer, R. L., Owens, S. E., and Rose, J. L., "Ultrasonic lamb wave tomography in structural health monitoring," *Smart Materials and Structures* **20**(10), 105002 (2011).

[2] Mallet, L., Lee, B., Staszewski, W., and Scarpa, F., "Structural health monitoring using scanning laser vibrometry: Ii. lamb waves for damagedetection," *Smart Materials and Structures* **13**(2), 261 (2004).

[3] Kudela, P., Radzienski, M., and Ostachowicz, W., "Impact induced damage assessment by means of lamb wave image processing," *Mechanical Systems and Signal Processing* **102**, 23–36 (2018).

[4] Růžek, R., Lohonka, R., and Jironč, J., "Ultrasonic c-scan and shearography ndi techniques evaluation of impact defects identification," *NDT & E International* **39**(2), 132–142 (2006).

[5] Cernadas, D., Trillo, C., Doval, A. F., López, O., López, C., Dorrío, B. V., Fernández, J. L., and Pérez-Amor, M., "Non-destructive testing of plates based on the visualisation of lamb waves by double-pulsed tv holography," *Mechanical systems and signal processing* **20**(6), 1338–1349 (2006).

[6] Müller, J., Geldmacher, J., König, C., Calomfirescu, M., and Jüptner, W., "Holographic interferometry as a tool to capture impact induced shock waves in carbon fibre composites," in [*Fringe 2005: The 5th International Workshop on Automatic Processing of Fringe Patterns*], 522–529, Springer (2005).

[7] Focke, O., Hildebrand, A., Von Kopylow, C., and Calomfirescu, M., "Inspection of lamb waves in carbon fiber composites using shearographic interferometry," in [*Nondestructive Characterization for Composite Materials, Aerospace Engineering, Civil Infrastructure, and Homeland Security 2008*], **6934**, 20–31, SPIE (2008).

[8] Lammering, R., "Observation of piezoelectrically induced lamb wave propagation in thin plates by use of speckle interferometry," *Experimental mechanics* **50**(3), 377–387 (2010).

[9] Zastavnik, F., Pyl, L., Gu, J., Sol, H., Kersemans, M., and Van Paepegem, W., "Comparison of shearography to scanning laser vibrometry as methods for local stiffness identification of beams," *Strain* **50**(1), 82–94 (2014).

[10] Wyant, J. C., "Use of an ac heterodyne lateral shear interferometer with real–time wavefront correction systems," *Applied optics* **14**(11), 2622–2626 (1975).

[11] Hariharan, P., Oreb, B. F., and Eiju, T., "Digital phase-shifting interferometry: a simple error-compensating phase calculation algorithm," *Applied optics* **26**(13), 2504–2506 (1987).

[12] Takeda, M., Ina, H., and Kobayashi, S., "Fourier-transform method of fringe-pattern analysis for computer-based topography and interferometry," *Journal of the optical society of America* **72**(1), 156–160 (1982).

[13] Anisimov, A. G. and Groves, R. M., "Extreme shearography: Development of a high-speed shearography instrument for quantitative surface strain measurements during an impact event," *Optics and Lasers in Engineering* **140**, 106502 (2021).

[14] Xie, X., Zheng, Y., Li, X., Sia, B., Zhong, P., Yang, G., and Yang, L., "Spatial phase-shift digital shearography for out-of-plane deformation measurement," *SAE International Journal of Materials and Manufacturing* **7**(2), 402–405 (2014).

[15] Gordon, G. A. and Mast, T. D., "Wide-area imaging of ultrasonic lamb wave fields by electronic speckle pattern interferometry," in [*Nondestructive Evaluation of Aging Aircraft, Airports, and Aerospace Hardware III*], **3586**, 297–309, SPIE (1999).

[16] Taillade, F., Krapez, J.-C., Lepoutre, F., and Balageas, D., "Shearographic visualization of lamb waves in carbon epoxy plates interaction with delaminations," *The European Physical Journal-Applied Physics* **9**(1), 69–73 (2000).

[17] Krapez, J.-C., Taillade, F., Lamarque, T., and Balageas, D., "Shearography: a tool for imaging lamb waves in composites and their interaction with delaminations," in [*Review of Progress in Quantitative Nondestructive Evaluation: Volume 18A–18B*], 905–912, Springer (1999).

[18] Xie, X., Li, J., Zhang, B., Yan, L., and Yang, L., "Improvement of phase map quality for michelson interferometer based spatial phase-shift digital shearography," *Asian J. Phys* **24**(10), 1391–1400 (2015).

[19] Pedrini, G., Zou, Y., and Tiziani, H., "Quantitative evaluation of digital shearing interferogram using the spatial carrier method," *Pure and Applied Optics: Journal of the European Optical Society Part A* **5**(3), 313 (1996).

[20] Bard, B. A., Gordon, G. A., and Wu, S., "Laser-modulated phase-stepping digital shearography for quantitative full-field imaging of ultrasonic waves," *The Journal of the Acoustical Society of America* **103**(6), 3327–3335 (1998).